

# A Machine Learning Paradigm for Studying Pictorial Realism: Are Constable's Clouds More Real than His Contemporaries?

Zhuomin Zhang, Elizabeth C. Mansfield, Jia Li, *Fellow, IEEE*, John Russell, George S. Young, Catherine Adams, and James Z. Wang

**Abstract**—European artists have sought to create life-like images since the Renaissance. The techniques used by artists to impart realism to their paintings often rely on approaches based in mathematics, like linear perspective; yet the means used to assess the verisimilitude of realist paintings have remained subjective, even intuitive. An exploration of alternative and relatively objective methods for evaluating pictorial realism could enhance existing art historical research. We propose a machine-learning-based paradigm for studying pictorial realism in an explainable way. Unlike subjective evaluations made by art historians or computer-based painting analysis exploiting inexplicable learned features, our framework assesses realism by measuring the similarity between clouds painted by exceptionally skillful 19th-century landscape painters like John Constable and photographs of clouds. The experimental results of cloud classification show that Constable approximates more consistently than his contemporaries the formal features of actual clouds in his paintings. Our analyses suggest that artists working in the decades leading up to the invention of photography worked in a mode that anticipated some of the stylistic features of photography. The study is a springboard for deeper analyses of pictorial realism using computer vision and machine learning.

**Index Terms**—Pictorial realism, John Constable, cloud classification, feature fusion, style disentanglement.

## 1 INTRODUCTION

LEONARDO da Vinci (1452–1519) once said “*The most praiseworthy form of painting is the one that most resembles what it imitates.*” Two celebrated inventions in Renaissance art—chiaroscuro and linear perspective—are for the purpose of faithfully representing reality on a two-dimensional picture surface. The former is the technique of using shading and highlights to convey the sense of volume for three-dimensional objects, and the latter is the mathematical system to create an illusion of space on a flat plane. Approaches to judging the verisimilitude of European paintings that aspire to represent reality are typically less methodical and more intuitive. This reliance on intuitive or instinctive judgments on the relative accuracy of painted scenes of observed nature is helpfully illustrated by an ancient Greek legend popular among Renaissance artists. According to the legend, the painter Apelles placed his life-size painting of a horse outdoors, eliciting appreciative whinnies from passing equines, thus proving its realism. This legend, as amusing as it is, nonetheless makes an important point about standards of judgment for pictorial realism.

In the past, assessments of realism in post-Renaissance paintings have relied on the opinions of art critics, art historians, and other interested viewers. These judgments are, of course, highly subjective insofar as they record the opinion of a particular viewer at a particular moment. The perceived fidelity of a painting to the natural phenomena it represents cannot always be clearly explained, because it is guided by an immediate, intuitive response to a particular painting. This is especially true of hard-to-describe phenomena like clouds or crashing waves: for most human viewers, paintings of these motifs simply “look right” or not (Fig. 1). Thus, developing AI-based methods for evaluating picturing realism objectively can greatly boost existing art historical research.

In this paper, we propose a new machine-learning-based paradigm for studying pictorial realism. The specific case study

in this paper is a comparison of paintings of clouds by John Constable (1776–1837) with those of his contemporaries, a research problem under current investigation by historians of European realist art. Although there is general agreement that Constable’s sky paintings are persuasive in their realism, the precise basis for his realism continues to be debated. Clouds are particularly hard to depict realistically, as American landscape painter Edgar Payne (1883–1947) explained [1]: “Of all outdoor motives, clouds and marines are the most difficult to draw and paint. Since clouds and water forms are constantly changing, there is not sufficient time for picturing.” This study of cloud paintings is thus a challenging case to test the machine learning paradigm. The feasibility of quantitative analysis for studying pictorial realism, as exemplified here, demonstrates that computational approaches may augment traditional approaches in new areas of art history.

### 1.1 The Art Historical Questions

Human viewers who have encountered post-Renaissance oil paintings executed in a naturalistic mode are habituated to the landscape genre and attribute varying degrees of realism to painted clouds without giving it much thought. For instance, in looking at depictions of clouds by British painter John Constable and French painter Eugène Boudin (1824–1898) that bear some similarity in terms of palette and general organization of atmospheric effects (Fig. 2), modern viewers typically feel confident rendering a judgment on which one seems more truthful. Yet, to what extent are the clouds convincing due to their painterly bravura, their reliance on pictorial structures we are accustomed to seeing as truthful, or their correspondence with embodied observations of meteorological phenomena? In seeking to answer these questions, art historians can augment documentary and material evidence



(a) John Constable, *Stormy Sea, Brighton*, circa 1828



(b) Gustave Courbet, *The Wave*, 1869

Fig. 1: Example paintings capturing hard-to-describe phenomena like clouds or ocean waves. (a) Oil on paper laid on canvas, (16.5 × 26.7 cm). Yale Center for British Art, New Haven. (b) Oil on canvas, (116.8 × 71.5 cm). Museum of Modern Art André Malraux.

with perceptual evidence achieved in part by becoming more aware of the acuity and limits of their own vision [2], [3], [4], [5].

In 1821, John Constable undertook a sustained campaign of “skying,” as he called his outdoor sketching of clouds. The significance of Constable’s interest in painting clouds has been debated. Some see the studies of this period as confirmation of the artist’s empiricism. Indeed, Constable noted date, time, and meteorological conditions on most of his painted cloud studies, lending credence to their exactitude. Yet faithful visual documentation of clouds is challenging because they are constantly changing. It seems reasonable to posit that Constable relied on certain artistic conventions or formal patterns as armatures for his paintings of these ever-shifting motifs as painters often did. It has also been argued that this phase of study was a belated response to Luke Howard’s classification of clouds into cumulus, cirrus, stratus, etc., a typology disseminated widely via the publication in 1803 of his *Essay on the Modifications of Clouds* [6], though there is no evidence that Constable owned or consulted Howard’s publication [7], [8], [9]. Other scholars have tended to shy away from attributing Constable’s remarkable realism to any single breakthrough, either conceptual or technical, preferring instead to attribute the artist’s achievement to a constellation of factors [9], [10], [11]. Whether guided by empirical study or artistic conven-

tion, some room for the exercise of the artist’s own imagination is readily acknowledged [11].

Based on these historical records and debates, our goal is to understand pictorial realism of Constable’s painted skies from two perspectives:

- 1) Do Constable’s clouds correspond with the system of cloud typology introduced in 1803 by Luke Howard?
- 2) How similar are the clouds painted by Constable and his contemporaries to photographs of real-world clouds?

By first establishing whether Constable’s clouds conform to the types described by Howard—a typology still in use today—we can begin to explore the possible relevance of the nascent science of meteorology for his understanding of the atmospheric phenomena he sought to depict in his paintings. Then, we exploit the extracted style information during the painting-photo translation process to quantitatively evaluate the style discrepancy between paintings and photos and among all different painters.

## 1.2 Overview of Our Approach

It is reasonable to assess the accuracy of a painting of a cloud by comparing it to a photograph of the same type of cloud. We thus propose to examine how well a collection of paintings of clouds can be categorized and how similar the styles of these paintings are in comparison with photos.

The whole pipeline of our proposed machine-learning-based method for studying pictorial realism is shown in Fig. 3, which consists of two parts, painted content classification and painting style evaluation. We first train a machine learning system to classify the categories using photographic images. For a set of paintings, we apply the classifier to predict their categories. In the meantime, classification labels are also created for the paintings by experts. Thus the classification accuracy for the paintings can be computed and compared with the accuracy achieved for photographs. Our basic assumption is that if the paintings imitate observed reality well, their classification accuracy will be close to that obtained for the photos. Further comparison can be conducted between different collections of paintings, allowing assessment of the relative fidelity to nature achieved in different sets. One typical case of comparison across collections is between the works of different artists. Then, we also train a style encoder during the disentanglement-based style transfer process. Next, we can compute the distance between encoded style features of the painted and real scene serving as another criterion to evaluate pictorial realism. In all, the proposed pipeline is designed to evaluate pictorial realism by accessing the similarity between paintings and photographs in terms of both the painted scene and painting style, which makes our evaluation system more thorough and unbiased.

For our study of Constable’s clouds, we rely on the expertise of a meteorologist to categorize clouds documented in photographs and paintings. The clouds are categorized into the types defined by Howard [6]. We propose a semi-supervised learning model for cloud classification in a feature fusion fashion using real-world photos. The classification of Constable’s clouds according to the standard typology allows for a more precise comparison of his clouds with those painted by his contemporaries. By comparing the class prediction of the AI system with ground truth labels created by a meteorologist, we obtain an objective assessment of the degree to which painters are differentiating cloud types



(a) John Constable, *Cloud Study*, 1822



(b) Eugène Boudin, *Beach Scene at Trouville*, 1863

Fig. 2: Example paintings used in our analysis to study painted clouds. (a) Oil on paper laid on panel, (28.6 × 48.3 cm). Yale Center for British Art, New Haven. (b) Oil on wood, (34.8 × 57.5 cm). National Gallery of Art, Washington.

(whether they are aware of the typology or not). In our scenario here, as highly specialized skills and knowledge are required to classify cloud types, the AI system cannot be replaced by an average human viewer. The supposition that Constable’s clouds strike viewers as more naturalistic because they do, in fact, conform to Howard’s now-standard typology is not predicated on viewers’ awareness of this. Then, we conduct a content-style-disentanglement-based image style transfer between paintings and photos to obtain the trained style encoder for each painter. We utilize the developed novel evaluation metrics for evaluating the discrepancy among these extracted style features of each painter’s collection to quantitatively show the influence of painting style on pictorial realism.

### 1.3 Contributions

The contributions of our work can be summarized as follows.

- We proposed a machine learning framework to study pictorial realism from an explainable and interdisciplinary perspective by leveraging computer vision techniques, meteorology expertise, and art history knowledge. Our work here aims at establishing a machine learning framework for a class of art historical research problems that are evident in the literature and under current investigation by seasoned researchers working in the field of European realist art. In this way, the work expands the applicability of machine learning for the study of art.
- We developed a new semi-supervised CNN model to achieve cloud type classification in a feature fusion fashion, named SFF-CNN. We proposed new evaluation metrics to access the style discrepancy between images.
- We curated a first-of-its-kind dataset containing 363 sky paintings from John Constable and six other influential contemporary painters. These paintings have all been professionally annotated by an expert meteorologist. This is the first usable annotated painting dataset prepared for computational sky painting analysis.
- With rigorous analysis, we provided strong scientific evidence to the art history community that systematic categorization is key for the visual impact of Constable’s realism in his cloud paintings. The study discovered a number of

other interesting findings that can be used by art historians to form hypotheses.

The rest of the paper is organized as follows. We discuss related work in Section 2. The data curation process is introduced in Section 3. The technical approach is described in Section 4. Experimental results are presented and analyzed in Section 5. Finally, we conclude in Section 6.

## 2 RELATED WORK

Literature on computational analysis of pictorial realism in paintings is scant. Here we briefly introduce some related work on AI-based painting analysis, art historical study of Constable’s skies, cloud classification modeling, and content-style disentanglement.

### 2.1 AI-based Painting Analysis

Existing research on AI-based painting analysis can generally be divided into two categories: 1) *understanding the content of paintings*: analyzing visual features for painting classification, painted content retrieval, picturing techniques analysis, among others, or 2) *creating the artworks*: computer-aided art generation of digital images for stylizing or creating new artworks for visualization and analysis.

CNN-learned features [12], [13] have often outperformed handcrafted features and been widely adopted for artist and genre classification tasks in recent years [14], [15]. Concurrently, other researchers focused on detecting figures and motifs or recognizing other depicted content in paintings with various supervised CNN models [16], [17]. In another approach, to generate a more comprehensive representation of paintings, Mao *et al.* proposed a unified retrieval system that learns a large number of features of artworks through a large-scale annotated painting dataset [18]. As for the quantitative analysis of visual features of paintings, Li *et al.* studied the painting styles of Vincent van Gogh by analyzing the attributes of brushstrokes extracted automatically with the help of edge detection and clustering-based segmentation [4]. Their techniques do not involve deep learning and are explainable. Shaik *et al.* tried to study style representations learned by a CNN architecture through combining other higher-level characteristics such as expert human knowledge and photo realism priors [19]. With the emergence of Generative Adversarial



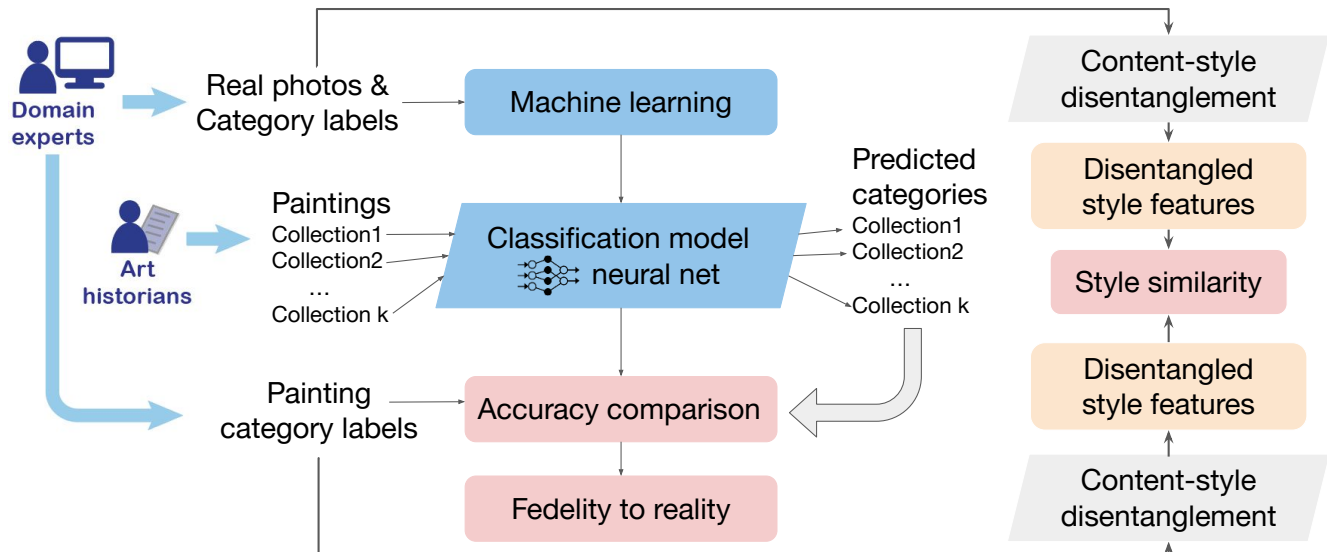


Fig. 3: The proposed machine-learning-based paradigm for studying pictorial realism.

Networks (GAN) [20], researchers have sought to create paintings based on this minimax optimization model. For instance, Kotovenko *et al.* achieved painting style transfer by incorporating the content and style disentanglement into the GAN framework [21]. Huang *et al.* tried to create paintings stroke by stroke with deep reinforcement learning [22]. For a more comprehensive review of the field of computerized analysis of paintings, readers are referred to a recent survey [5].

However, most existing AI-related analyses and creations of paintings cannot provide sufficient interpretability, substantially limiting their acceptance and utility in the field of art history [23]. The topics related to semantic demonstration of characteristics of paintings are treated superficially and painting collections are just regarded as another source of image datasets for computational analysis. The goal of computational analysis of artworks is actually a complex topic that often relies upon knowledge from other research fields because the extracted CNN features are often impossible to explain in a way useful to art historians. Therefore, we attempt to solve the pictorial realism evaluation problem in an explainable fashion by comparing John Constable’s clouds with those of his contemporaries using art historical and meteorological knowledge, in addition to CNN-based image classification.

## 2.2 Constable’s Clouds

Modern art historical scholarship on Constable’s clouds began with Kurt Badt’s 1950 book on the subject [7]. Prior to this, accounts of Constable’s clouds were largely descriptive as opposed to analytical, attributing their naturalism to Constable’s emotional connection with nature, his devotion to sketching outdoors, or his largely rural childhood [8]. Badt was the first to argue that Constable’s proficiency with painting naturalistic clouds was due to his familiarity with the recent development of a taxonomy of clouds created by British chemist Luke Howard. Howard’s taxonomy was published in 1803 and was widely disseminated during Constable’s lifetime, so it was available to him. But there is no evidence that Constable possessed it, and the artist’s extant correspondence and other documents make no direct reference to Howard [9]. More recent scholars tend to cite instead Constable’s dedication to sustained periods of empirical observation of

clouds [10], [11] and his familiarity with earlier paintings of naturalistic landscapes by artists like Claude Lorrain or Willem van de Velde the Younger, both of whom were well represented in English collections during Constable’s lifetime [9], [24]. In addition, a Romantic explanation for Constable’s naturalism likewise persists in the scholarly literature to this day, attributing his naturalism at least in part to an emotional or spiritual impulse toward accuracy in his depictions of natural phenomena [25].

## 2.3 Semi-supervised Cloud Classification

The meteorological field of atmospheric dynamics encompasses the study of weather, including such phenomena as clouds. Accurate cloud type classification is important for research such as radiative transfer and solar energy estimation [26]. In our case, the accuracy of cloud type classification is regarded as strong evidence of persuasive pictorial realism, so building a trustworthy cloud type classifier is indispensable. As human labeling is inaccurate unless performed by an expert meteorologist and, even then, is inefficient, automatic cloud type classification has developed as a computer vision research direction in recent years. Most existing cloud classification methods can be categorized into: 1) handcrafted feature extraction and 2) learned features from CNN modeling. For the first type, texture or spectral feature extraction [27], [28], [29] are common approaches for cloud classification, but these low-level feature-based algorithms cannot produce high accuracy. Dev *et al.* attempted to integrate both color and texture information to improve the results, but the dataset they collected is too limited to make the results convincing [30]. Recently, researchers have started to adopt CNNs on their cloud classification tasks. Zhang *et al.* built a larger ground-based cloud dataset, called Cirrus Cumulus Stratus Nimbus (CCSN), which consists of 11 categories of clouds under meteorological standards and proposed a new CNN model, called CloudNet, for accurate ground-based meteorological cloud classification [31]. Huertas *et al.* then proposed a feature fusion model combining CNN features and handcrafted low-level textural features to boost the classification results [32].

Different from this fusion model, our approach aims at extracting more task-relevant features such as the cloud contours

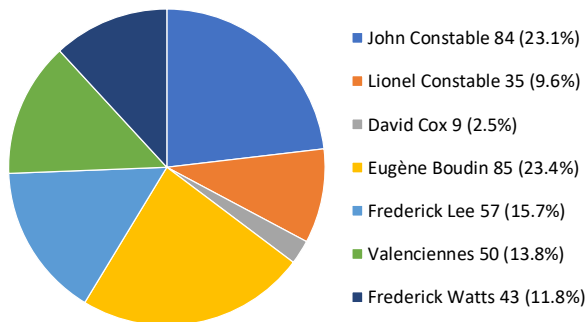


of clouds for the fusion to improve the classification accuracy on both the photo and painting datasets. Another problem we need to resolve to build a more robust classification model is the deficiency of labeled cloud photos. The emergence of semi-supervised learning can greatly boost classification performance by utilizing a great amount of unlabeled data during the training process. The common semi-supervised classification models can be categorized into self-training [33], co-training [34], graph-based semi-supervised learning [35], and semi-supervised supported vector machine [36]. In our case, we generate pseudo labels for two unlabeled sky photo datasets and then add these new data to the labeled CCSN dataset to realize dataset expansion.

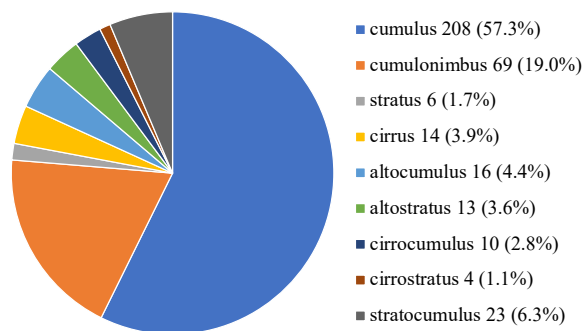
## 2.4 Content Style Disentanglement

Content-style disentanglement is extensively utilized for feature coupling in many applications, such as semantic segmentation [37], pose estimation [38], and image style transfer [39], [40], [41], where both the content and style feature representations can be used separately for downstream problems. In image translation, most CNN-based methods aim to learn latent space representations by extracting content or style information using auto-encoder variants. Some evaluation metrics such as correlation and informativeness have been proposed to quantitatively assess the performance of the disentanglement itself [42]. However, utilizing these disentangled features for similarity or discrepancy comparison among paintings from different painters has not been explored.

## 3 REALISM PAINTING DATASET



(a) by artist



(b) by cloud type

Fig. 4: Painting dataset distributions. John Constable and Boudin’s paintings have the highest percentages in the dataset. Cumulus and cumulonimbus are the two most dominant cloud types.

We carefully curate a dataset of oil paintings by John Constable and six of his near-contemporaries: Pierre Henri de Valenciennes (1750-1819), John Constable (1776-1837), David Cox (1783-1859), Frederick Richard Lee (1798-1879), Frederick W. Watts (1800-1870), Eugène Boudin (1824-1898), and Lionel Constable (1828-1887). All of these images are either high-resolution scans of existing reproductions or digital photographs of landscape paintings with “finished” clouds or pure cloud studies. Here are the key factors we use to select proper artistic works for comparison:

- We should maintain a dataset that is consistent in terms of medium. In other words, since Constable painted with oil rather than watercolor, we should find comparative works that are also oil paintings.
- It can be hard to know for certain that a cloud study was entirely executed outdoors or touched up in the studio, so we should use artists who worked out-of-doors as well as in the studio.
- We should use artists for whom clouds were a sustained concern, since this may result in a larger dataset as we can collect more paintings for one painter.

In our dataset, all these artists worked in oil and all had long engagement with sky/clouds. For instance, Lionel, son of John Constable, sought to emulate his father’s technique for a very long time; French artist Eugene Boudin was known as “king of skies” [43] and encouraged a number of artists like Courbet and Monet to paint clouds en plein air; Valenciennes, trained younger artists to paint out of doors and to work on cloud studies. Other painters in our dataset were also experienced in sky/clouds paintings.

Along with these carefully-collected paintings, cloud types of each painting are also expertly labeled by a meteorologist with expertise in atmospheric dynamics who also possesses basic knowledge of the history of European landscape painting. Annotations by the meteorologist indicate not only cloud type, but also include some more detailed meteorological information, including the cloud structure, apparent weather conditions, etc. Finally, a dataset containing 363 images with detailed labeled metadata is established for our work, which can be further used for the deeper relation analysis between painted clouds and meteorological phenomenon. Fig. 4 shows the painting distribution in our dataset in terms of painters and cloud types. As can be seen, there are more Boudin’s and John Constable’s and more cumulus paintings in our dataset.

## 4 METHOD

### 4.1 A New Paradigm for Studying Pictorial Realism

The proposed paradigm, as illustrated in Fig. 3 and outlined in Section 1.2, provides an unprecedented perspective for comparing artworks and addresses the subjectivity of experts’ opinions. Intuitively, if we want to assess whether a painting accurately captures the real scene, we can compare the painting with a photo taken of the same scene at the same time. However, this approach is clearly unfeasible for paintings made in the past, not to mention incompatible with the European aesthetic doctrine that the ultimate goal of art is not to merely duplicate nature. What is more, for paintings that depict outdoor scenes, it is simply impossible to stage an approximate scene because of the complexity and vast scales of natural objects, *e.g.*, clouds, trees, and the richness and perplexing characteristics of outdoor lighting and atmospheric

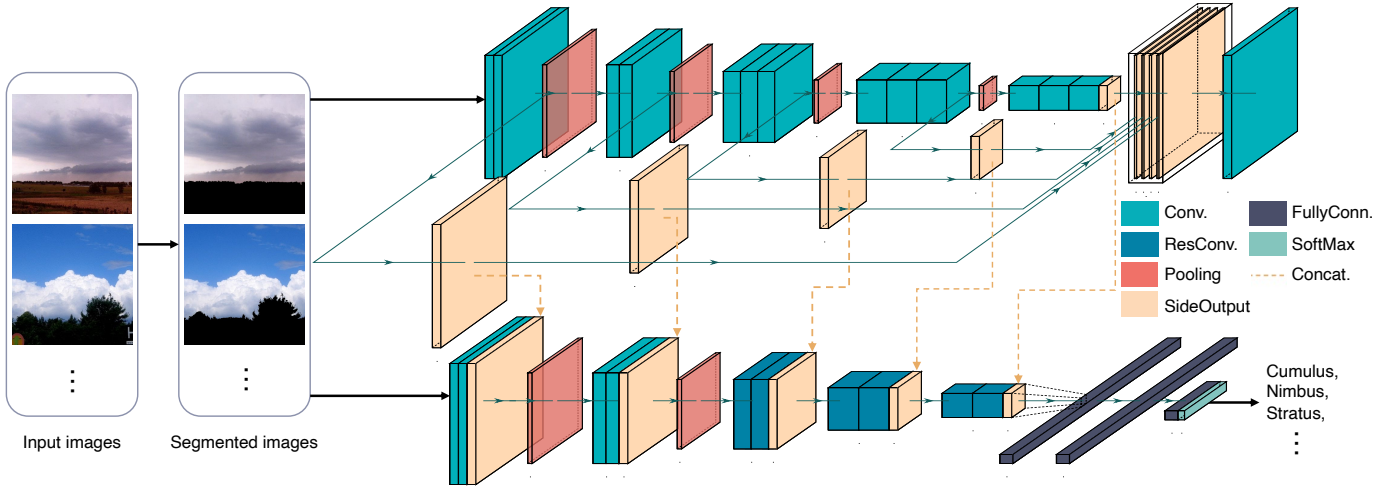


Fig. 5: The structure of our cloud classification. First, we need to get segmented images to use as input to the network. Then, two streams of encoders aim for extracting classic and edge features.

conditions. We thus propose to categorize a natural phenomenon—clouds—and examine how well a collection of paintings of clouds can be categorized in comparison with photos.

## 4.2 Semi-supervised Cloud Classification

Our classification model consists of two main steps: clustering-based sky segmentation and classification by a *semi-supervised feature fusion CNN (SFF-CNN)* model, as shown in Fig. 5. The sky segmentation step reduces the impact of irrelevant parts of an image on classification. SFF-CNN contains two streams of feature extraction, aptly called the *classic feature extractor* and *edge feature extractor*. The former generates features from low-level textures or patterns to high-level object-related characteristics, while the latter focuses on edge information. The fused features from the two encoders are utilized together for the ultimate class label prediction. We are motivated to extend a typical CNN model by incorporating edge features because the contour information of cloud bases and upper draft turrets is an important factor for meteorologists to determine the type of cloud. This classification is also exploited to generate pseudo labels during the semi-supervised learning process.

The detailed algorithms for sky segmentation and CNN-based cloud type classification model are illustrated in the following.

### 4.2.1 Sky Segmentation

The land, mountain, or other irrelevant regions in a painting can negatively interfere with the image classification performance. Because our study focuses on the sky regions for feature extraction, we eliminate the impact of other irrelevant parts in the paintings. That is, the pixels out of the sky region should be excluded from the subsequent classification model. We used the Agglomerative Connectivity Constrained Clustering (A3C) algorithm [44] to segment images. The method combines top-down multi-depth k-means clustering and a bottom-up agglomerative connectivity constrained merging method. Features defined based on color, edge, locations, balance, and jaggedness of boundaries are used to merge relatively homogeneous and local patches into segments. In our case, we first obtain the segments through the A3C algorithm and then apply a logistic regression on the location and color

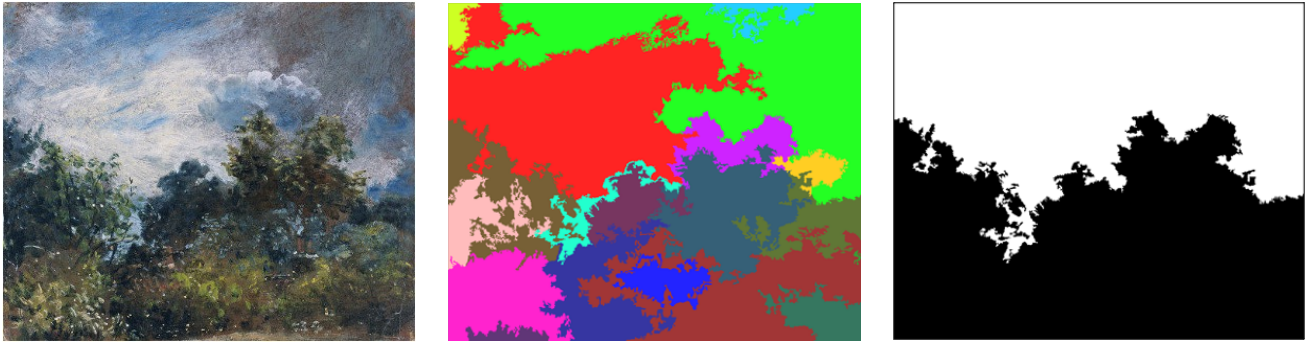
features extracted from each segment to realize a two-class sky-land segmentation.

The segments obtained by the A3C algorithm are usually more fragmented than semantic regions (*e.g.*, sky, trees, land). Since our purpose is to extract the sky region for the subsequent cloud type classification, we further label segments in an image as sky versus land or other irrelevant objects using a two-class logistic regression classifier. Through the experiment, we notice that location and color-based features can have a significant impact on the regression performance, thus for each segment, a 10-dimensional feature vector is computed. Specifically, these features include *normalized intensity, normalized saturation, normalized hue, the square of intensity, the square of saturation, the cosine of the average hue, average vertical position, top-most vertical position, bottom-most vertical position, and the ratio between width/height by bounding box*. Fig. 6 shows the clustering results of three example images, including two paintings and one photograph, and the sky versus non-sky classification results of the segments. To counter adversarial effects of non-sky regions while classifying the cloud types by the CNN model, the entire non-sky region of a painting image is replaced by black pixels and the modified image becomes the input to the CNN model, which we refer to as the *sky-selected image*.

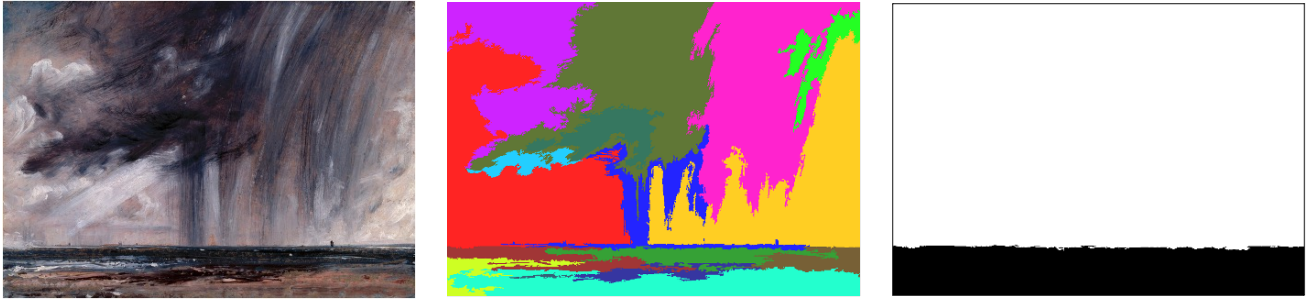
### 4.2.2 Cloud Classification

The sky-selected images are classified into different cloud types by the feature fusion CNN model. Our neural network is custom-designed for the cloud classification task by incorporating pre-learned edge features into the layers of a typical CNN model (Fig. 5). The neural network consists of a bottom stream for classic feature extraction and a top stream for edge feature extraction. The classic feature extractor aims at extracting useful features from low-level textures or patterns to high-level object-related quantities, while the edge feature extractor only captures the characteristics of edges in the same input image. Both feature extractors take the three-color-channel sky-selected images as the input. Denote the  $k$ th sky-selected image by  $\mathbf{I}_k$ .

**Classic Feature Extraction:** The encoder for classic feature extraction takes the three-color-channel sky-selected paintings  $\mathbf{I}_k$  as the input. The first two convolutional blocks both consist of



(a) John Constable, *Study of Sky and Trees*, 1821

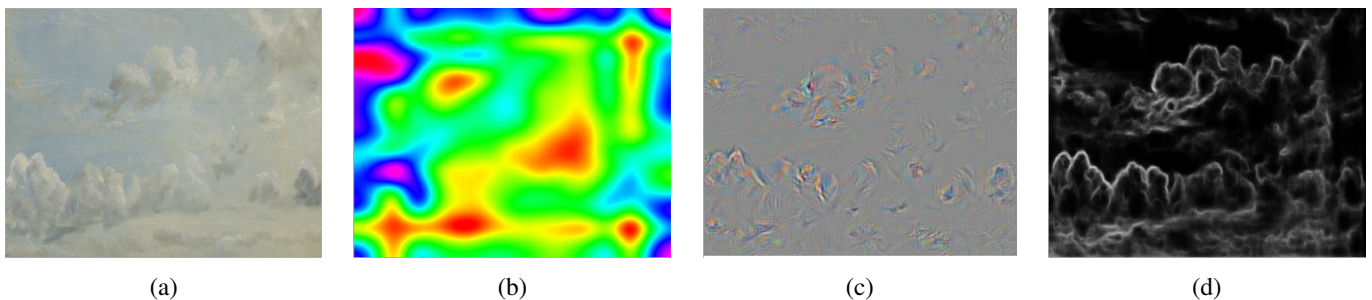


(b) John Constable, *Rainstorm over the Sea*, circa 1824-1828



(c) A photo of real-world cloud from the CCSN dataset

Fig. 6: Sky and ground segmentation illustrated with three examples. Left: Original painting or photo. Middle: Segments generated after a two-round merging. Right: Sky and land segmentation maps.



(a)

(b)

(c)

(d)

Fig. 7: Grad-Cam visualization. (a) Example cloud painting. (b) The Grad-Cam heatmap highlights where the model relies on most to conclude the class of the image. Warmer colors indicate a higher significance of a location in the feature map. Red is the warmest, with yellow, green, blue, purple becoming increasingly cooler. (c) The guided back-propagation plot is another way to show the contribution of features to the classification result. Brighter pixels indicate that the features at their positions are more important. (d) The output edge estimation of the HED model.



two Conv-BatchNorm-Relu layers and are followed by a  $2 \times 2$  pooling layer to downsample the input feature maps. The convolutional layers in these two blocks all have stride 1 and the kernel size is  $3 \times 3$ . The next two blocks are residual blocks with two convolutional layers using stride 1 and 2 respectively and the same kernel size  $3 \times 3$ . Each of these blocks spatially downsamples the input feature maps to half of their size. The residual structure has been shown particularly helpful for training deep architectures [45]. The third residual convolutional module follows the same structure as the first two but uses stride 1 for both of the convolutional layers. Then three fully-connected layers are connected to the Resconv modules. The final layer of Softmax activation produces a distribution over the 10 output probability classes for each category. Lastly, the cross-entropy (CE) loss [46] is applied to train the network.

**Edge Feature Extraction:** To find what features are most important for the CNN classification model, we use the Grad-cam visualization method [47], which provides a heatmap indicating the significance of any location in the feature map for reaching the classification decision. In Figures 7 (b) and 7 (c), the visualization result for an example image based on the final convolution layer in the last Resconv module shows that the edge information of each cloud mass is important for classifying the cloud type. We are thus motivated to directly include edge- or contour-related features in the neural network in order to increase classification accuracy. Indeed, experiments show that the strategy to fuse edge features in the CNN has yielded better classification (Fig. 10). Specifically, we compute the edge features by a pre-trained encoder named holistically-nested features for edge detection (HED) [48]. An example output of the HED is shown in Fig. 7 (d). The side-output layer of each convolution module of HED generates an edge feature map at a particular receptive field size, denoted as feature maps  $\{f_1^e, f_2^e, f_3^e, f_4^e, f_5^e\}$ , which are concatenated with the feature maps generated by the CNN at corresponding layers. By concatenation, we mean that features at any location in one map are expanded with features at the same location in another map. The two feature maps are ensured to have the same size (horizontally and vertically) such that the correspondence between locations is obvious. In particular, we use the same setting for the HED and CNN architectures so that at every layer, their respective feature maps are generated with the same receptive field size. The augmented feature map at the  $i$ th layer, denoted by  $f_i^f$ , is the input to the next convolution layer.

### 4.2.3 Semi-supervised Learning

To further enhance cloud classification accuracy, we employ semi-supervised learning to leverage a large set of unlabeled cloud photos. We selected 9883 images from SkyFinder dataset [49] and FindMeASky dataset [50] as unlabeled data. Specifically, we follow the approach of FixMatch [51]. For each unlabeled image, we create the image by the flipping and shifting operations. This version is called a weak augmentation image. Additionally, another version of the image, called a strong augmentation image, is created by another two operations, namely, CTAugment followed by Cutout [51]. We apply the classifier trained using only the labeled images to classify the weak augmentation images. The class that has the maximum predicted posterior probability is chosen as the predicted class (also called the one-hot pseudo label). To counter the negative effect of possibly incorrect pseudo labels, the maximum predicted posterior is compared with a pre-chosen threshold. If the threshold is not exceeded, this unlabeled image

and its augmented versions will not be used further. Otherwise, the pseudo label is treated as the true label for the strong augmentation images, which we refer to as high-confidence unlabeled images. Finally, another round of training is performed using both labeled images and the high-confidence unlabeled images. The cross-entropy between the true class (or pseudo-class in the case of unlabeled images) and the predicted class posteriors is defined as the loss induced by that image. Let the average loss for the labeled images be  $L_l$  and that for the high-confidence unlabeled images be  $L_u$ . Then the overall loss used to retrain the classifier is  $L = L_l + \alpha L_u$ , where  $\alpha$  is a pre-selected hyperparameter.

## 4.3 Style Disentanglement

To evaluate pictorial realism, in addition to comparing paintings based on how well they can be classified, we propose a pipeline for assessing similarity between the so-called “style” features of pictures. In MUNIT [52], an image is decomposed into two representation parts—content versus style. Both the content and style features are extracted by an encoding CNN, and they can be combined as input to a decoding CNN to recover the original image. Roughly speaking, the content features capture the shared characteristics of two groups of images, whereas the style features capture the distinct characteristics of each group. The encoders and decoders for the two groups of images are trained together to ensure that the content features correspond to traits shared by the two groups. We are motivated to separate content and style computationally because we cannot collect paintings depicting the same objects by different artists. As a result, it is questionable whether any measure of the difference between two groups of pictures is caused by the painted objects or by the painting techniques or styles of the artists.

A schematic plot for the extraction of content and style features by MUNIT [52] is given in Fig. 8. In our analysis, we treat the set of paintings of every artist as domain  $\mathcal{A}$  and the set of real photos as the reference domain  $\mathcal{P}$ . This training process yields a content encoder and a style encoder for each artist. The training algorithm generates photo-like images  $I_{\mathcal{A}2\mathcal{P}}$  from images in domain  $\mathcal{A}$  or painting-like images  $I_{\mathcal{P}2\mathcal{A}}$  from those in domain  $\mathcal{P}$ , an operation called “cross-domain style translation”. The translation is realized by keeping the content features but adopting style features generated for an image in the other domain. These cross-domain features are input to a decoder to reconstruct a translated picture. We refer to [52] for more details. The training objective function used in [52] has been modified slightly in [42] by removing the learning regression loss because the authors of the latter found that better separation of content and style can be obtained and more correlated the style and input image will be. In the discussion below, we refer to the style features computed based on a style encoder simply as the “style” of an image. We compare the painting styles between artists as well as between every artist and the real photos.

### 4.3.1 Style Similarity Between Artists

First, to evaluate style similarity between artists, we consider two groups of paintings denoted by group  $\mathcal{A}$  and  $\mathcal{B}$ . Suppose  $\mathcal{A} = \{a_i : i \in (1, 2, \dots, n_A)\}$  contains  $n_A$  pictures and  $\mathcal{B} = \{b_j : j \in (1, 2, \dots, n_B)\}$  contains  $n_B$  pictures. Denote the content and style encoder trained based on style transfer from painting group  $\mathcal{A}$  to photo group  $\mathcal{P} = \{p_k : k \in (1, 2, \dots, n_P)\}$  by  $E_C^{\mathcal{A}}$  and  $E_S^{\mathcal{A}}$  respectively. Likewise, the encoders for  $\mathcal{B}$  are  $E_C^{\mathcal{B}}$  and  $E_S^{\mathcal{B}}$ .

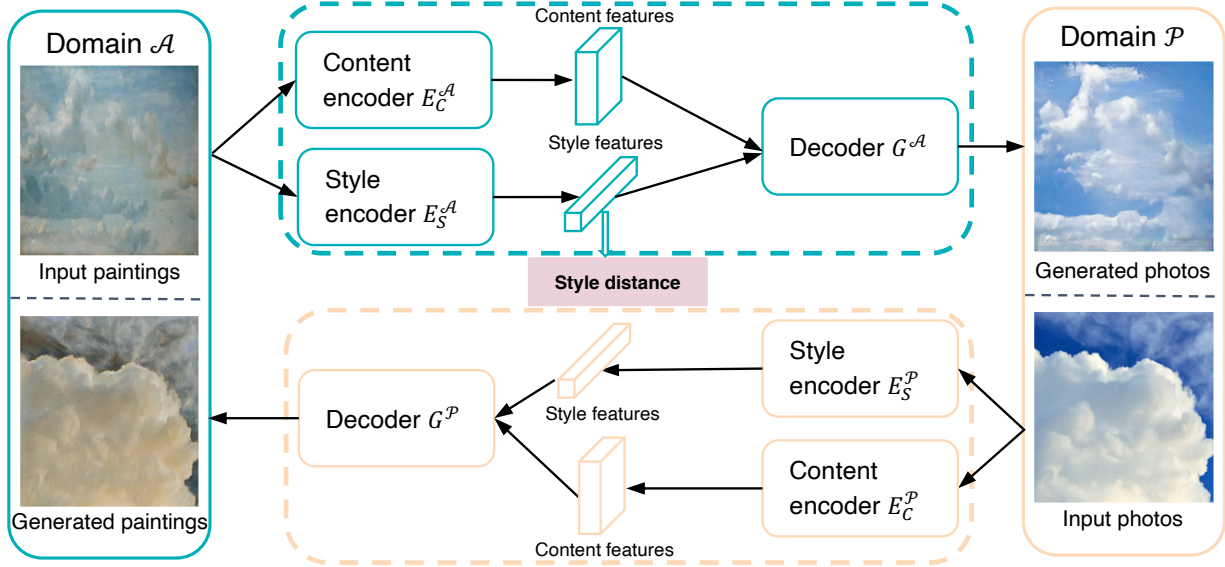


Fig. 8: The process of image translation from paintings to real photos with content-style disentanglement.

For an image  $a_i \in \mathcal{A}$ , denote its style features computed by  $E_S^{\mathcal{A}}$  by  $F_S^{a_i}$ . Similarly, for any  $b_j \in \mathcal{B}$ , let its style computed by  $E_S^{\mathcal{B}}$  be  $F_S^{b_j}$ . If  $\mathcal{A}$  and  $\mathcal{B}$  are similar in style, we would expect  $F_S^{a_i}$  and  $F_S^{b_j}$  to be close on average. Use the normalized square of the  $L_2$  norm of a style feature vector to indicate the signal strength:  $I_S^{a_i} = \|F_S^{a_i}\|^2/d$ , where  $d$  is the dimension of the style feature vectors. The Mean Squared Error (MSE) between  $F_S^{a_i}$  and  $F_S^{b_j}$  is simply  $\|F_S^{a_i} - F_S^{b_j}\|^2/d$ . For each image  $a_i \in \mathcal{A}$ , we define its average distance to images in  $\mathcal{B}$  by

$$D_{\mathcal{A}}^{a_i} = \frac{1}{n_B} \sum_{b_j \in \mathcal{B}} \frac{\text{MSE}(F_S^{a_i}, F_S^{b_j})}{I_S^{a_i}}. \quad (1)$$

Conversely, for each image  $b_j \in \mathcal{B}$ , we define its average distance to images in  $\mathcal{A}$  by

$$D_{\mathcal{B}}^{b_j} = \frac{1}{n_A} \sum_{a_i \in \mathcal{A}} \frac{\text{MSE}(F_S^{b_j}, F_S^{a_i})}{I_S^{b_j}}. \quad (2)$$

Finally, define

$$\begin{aligned} D_{\mathcal{A}} &= \frac{1}{n_A} \sum_{a_i \in \mathcal{A}} D_{\mathcal{A}}^{a_i}, \\ D_{\mathcal{B}} &= \frac{1}{n_B} \sum_{b_j \in \mathcal{B}} D_{\mathcal{B}}^{b_j}, \\ D_{\text{style}}(\mathcal{A}, \mathcal{B}) &= \frac{1}{2}(D_{\mathcal{A}} + D_{\mathcal{B}}). \end{aligned} \quad (3)$$

The distance  $D_{\text{style}}$  is taken to measure the style difference between group  $\mathcal{A}$  and  $\mathcal{B}$ .

#### 4.3.2 Style Similarity Between an Artist and Photos

Next, we propose to use the metric ‘‘Information Over Bias (IOB)’’ [42] to measure the difference between the paintings of an artist and real photos. For an image  $a_i \in \mathcal{A}$ , where  $a_i$  is treated as a vector, let its style feature vector be  $F_S^{a_i}$ .  $\text{IOB}(a_i, F_S^{a_i})$  is defined to quantify the amount of information in  $a_i$  which is captured by  $F_S^{a_i}$ . Specifically, the informativeness of  $F_S^{a_i}$  is measured by the ratio between  $\text{MSE}(a_i, \tilde{a}_i')$  and  $\text{MSE}(a_i, \tilde{a}_i)$ ,

where  $\tilde{a}_i'$  is a reconstructed image from an uninformative constant substitute style vector  $\mathbb{1}$  combined with  $a_i$ 's content feature vector, while  $\tilde{a}_i$  is generated from the informative style vector  $F_S^{a_i}$  and the same content vector. Thus we define  $\text{IOB}(a_i, F_S^{a_i})$  by

$$\text{IOB}(a_i, F_S^{a_i}) = \frac{\text{MSE}(a_i, \tilde{a}_i')}{\text{MSE}(a_i, \tilde{a}_i)}. \quad (4)$$

With a slight abuse of notation, we also use  $\text{IOB}(\mathcal{A})$  to denote the average IOB values for the images in  $\mathcal{A}$ :

$$\text{IOB}(\mathcal{A}) = \frac{1}{n_A} \sum_{i=1}^{n_A} \text{IOB}(a_i, F_S^{a_i}). \quad (5)$$

A lower value of  $\text{IOB}(\mathcal{A})$  indicates that the style representation of the image is less important since a substitute default style vector can result in reconstruction with a similar level of disparity from the original image. Because the style feature vectors capture the distinct characteristics of one group of images from another group, less informative style vectors reflect a higher similarity between the two groups of images. To form a basis of comparison, we also compute IOB for a mixed group containing both paintings and real photos. Specifically, we first compute  $\text{IOB}(\mathcal{A})$  for a group of paintings by an artist using the style transfer process from paintings to photos. Then we mix images from the painting group  $\mathcal{A}$  and the photo group  $\mathcal{P}$  to form a new group  $\mathcal{M} = \{a_i : i \in (1, 2, \dots, n_A), p_k : k \in (1, 2, \dots, n_P)\}$ . Again by the style transfer process from group  $\mathcal{M}$  to  $\mathcal{P}$ , we can compute  $\text{IOB}(\mathcal{M})$ . Finally, the style distance between an artist and the real photos is defined as the following ratio:

$$R_{\text{style}}(\mathcal{A}) = \frac{\text{IOB}(\mathcal{M})}{\text{IOB}(\mathcal{A})}. \quad (6)$$

## 5 EXPERIMENTAL RESULTS

In this section, we first provide results to demonstrate that our cloud classification model outperforms the state-of-the-art models. This fact justifies our usage of the AI system to provide a high-quality assessment of the similarity between clouds in the

TABLE 1: Descriptions of different cloud formations in the CCSN dataset.

Cloud Level	Cloud Genus	Abbreviation	Characteristics	Number of Images
High level	Cirrus	Ci	Fibrous, thin, white and transparent clouds	139
	Cirrocumulus	Cc	Small and white flakes arranged in groups	268
	Cirrostratus	Cs	Thin and translucent ice crystals	287
Mid level	Alto cumulus	Ac	Thicker and grey line-arranged cloud sheets	221
	Altostratus	As	Opaque striped veil of greyish cloud	188
Low level	Stratus	St	Ragged and stratiform clouds that lay evenly	202
	Stratocumulus	Sc	Dark grey layered clouds	340
	Nimbostratus	Ns	Deep grey and fluffy rain clouds	274
Vertical level	Cumulus	Cu	Greyish clouds with clear contours, flat bases and circular tops	182
	Cumulonimbus	Cb	Dark-grey rain clouds with blurry and doomed edges	242

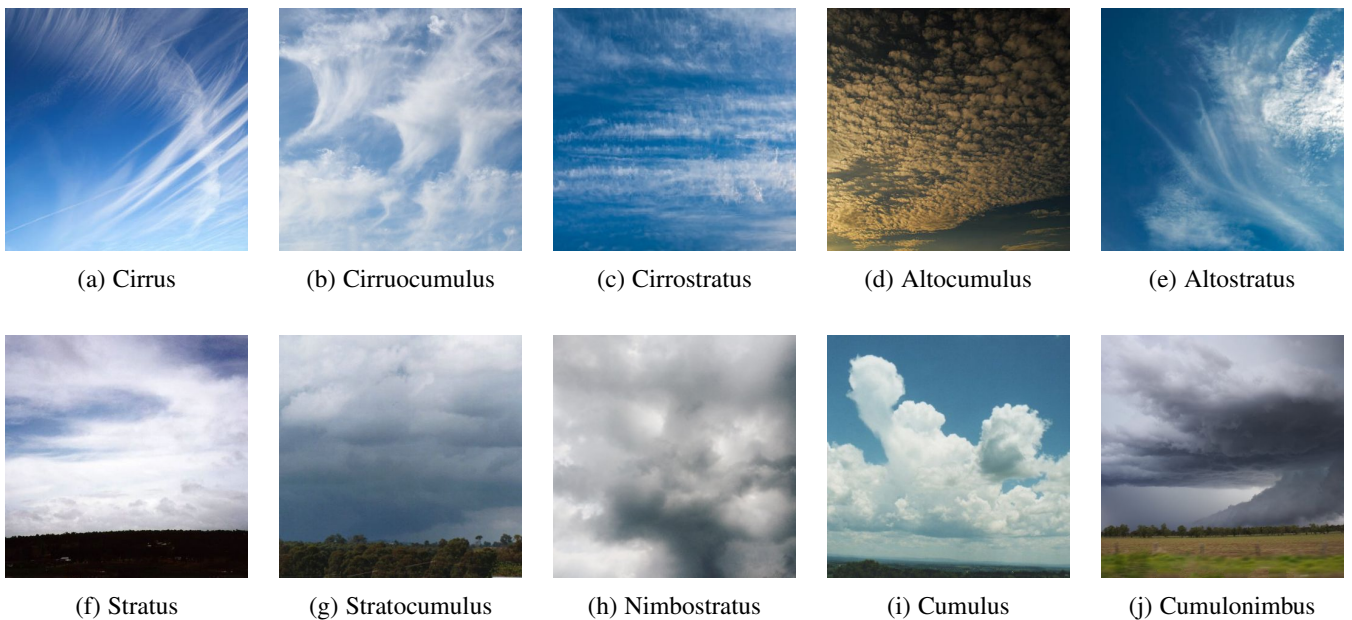


Fig. 9: Representative photographs of different types of clouds in the CCSN dataset.

paintings and those in real photos. We will then compare the cloud classification accuracy achieved for the paintings of each artist and conduct hypothesis testing to investigate whether the difference between artists is statistically significant. Furthermore, we show the statistics represent the style similarity between paintings of each painter and real photos and style discrepancy among paired painters.

## 5.1 Cloud Photo Dataset

To evaluate the accuracy of sky segmentation and the classification performance on the sky photos, we adopt the CCSN dataset for training and testing. The CCSN dataset contains 2543 cloud images in total. According to the World Meteorological Organization’s genera-based classification recommendation, all the collected images are divided into 11 different categories as shown in Table. 1. Representative sample images from each category are shown in Fig. 9. All images are fixed resolution  $400 \times 400$  pixels in the JPEG format. It is worth noting that we exclude the class “contrails” during the training phase since there are no contrails appearing in the collected paintings, so we formulate this

could type identification problem as a 10-class image classification work.

To realize semi-supervised learning, we leverage the SkyFinder [49] and FindMeASky [50] datasets to boost the classification performance. The SkyFinder dataset contains over 90,000 outdoor sky photos in different weather situations with associated detailed weather data and annotated sky pixels. However, not all photos were taken in a cloudy situation and there are plenty of photos shot in repetitive views, so we only use 3,204 images from this dataset by only keeping images labeled as “cloudy” and eliminating images taken from the same camera and on the same day. In addition, the FindMeASky dataset consists of 6,679 outdoor sky images with corresponding binary masks filtered from ADE20K Dataset [53] where the sky region occupies over 40% region of the whole image. Therefore, our unlabeled dataset has 9,883 images in total.

## 5.2 Classification Result on Cloud Photos

To show the reliability and robustness of our segmentation algorithm, we randomly selected 20% of the images from the painting



dataset for testing and manually labeled sky and ground regions to be used as the ground truth. To measure the accuracy of sky segmentation, we computed pixel accuracy, mean accuracy, and mean IoU as the evaluation metrics [54], which are 0.9912, 0.9723, and 0.9532, respectively. These accuracy values are regarded as high.

To evaluate the classification performance, we randomly selected 20% of the images from the CCSN dataset for testing. The other 80% labeled images from the CCSN dataset and all the unlabeled images are used together during the self-training process. Data augmentation methods such as random flipping, and shifting [55] are adopted as weak augmentation. As for the feature extraction module, we use the pre-trained model described in the original paper with the default hyperparameters. Only the parameters in the encoder for classic feature extraction are learned and adjusted in the training process. The CNN is trained with a stochastic gradient and running on an NVIDIA GeForce GTX2080i with batch size 16. As mentioned before, there are 10 cloud types. We compared the classification results obtained by our model with or without feature fusion, with or without semi-supervised learning, and another two advanced methods: CloudNet [31] and ensemble-learning-based classification [32]. The classification performance is evaluated using standard evaluation metrics, including precision, recall, and accuracy [56]. Table 2 shows the averages of these evaluation metrics across the cloud categories. Since the codes for both these two methods are not available, we re-implemented the proposed method using the network structure described in the papers. The accurate values of some hyperparameters are not listed in the papers, so the results may have some deviations from the originally reported results. All the evaluation metrics are averaged by cloud category. The feature fusion semi-supervised model achieves the best performance with a precision of 0.986, recall of 0.953, and accuracy of 0.966. Except for exploiting unlabeled data, the improvement of the classification accuracy of our feature fusion model can be credited to 1) sky segmentation which removes the interference of irrelevant regions and 2) the fused edge features which help identify some contour-sensitive cloud types.

TABLE 2: The classification results of each model.

Method	Precision	Recall	Accuracy
CloudNet [31]	0.891	0.868	0.875
Ensemble Learning [32]	0.953	0.902	0.937
Ours (w/o feature fusion)	0.947	0.908	0.933
Ours (with feature fusion)	0.961	0.922	0.949
Ours-semi (w/o feature fusion)	0.977	0.931	0.962
Ours-semi (with feature fusion)	<b>0.986</b>	<b>0.953</b>	<b>0.966</b>

### 5.3 Classification Result on the Paintings

After verifying that the trained classification model can achieve satisfactory performance, we re-trained the classification model on the entire CCSN dataset, which was then applied to the paintings. Because the painting dataset is small and the prevalence of different cloud types is highly unbalanced, in the discussion of classification accuracy for the painting dataset, we only discriminate at the granularity of five common cloud types: cumuliform (cumulus), cumulonimbiform (cumulonimbus), cirriform (cirrus), stratiform (stratus, cirrostratus, altostratus, and nimbostratus), and

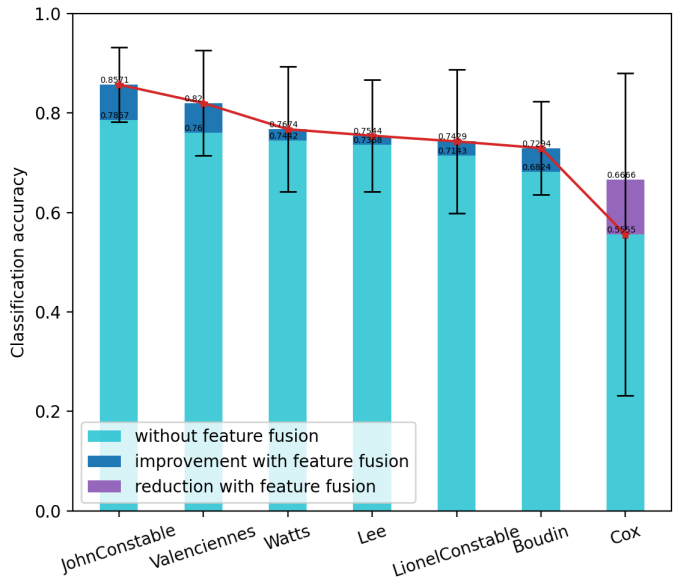


Fig. 10: The comparison in terms of classification accuracy of all seven painters using the CNN model with or without feature fusion. The error bars denote the confidence interval for the classification accuracy at the significance level 0.05 of each painter.

stratocumuliform (cirrocumulus, altocumulus, and stratocumulus) [57]. The classification accuracy of each painter using the semi-supervised CNN model with or without feature fusion is shown in Fig. 10. For the accuracy achieved with feature fusion, the confidence interval for the accuracy at significance level 0.05 is shown. Except for Cox, all the other artists have confidence intervals of accuracy completely above 60% (higher than the percentage of the most dominant cloud type), indicating that the clouds they painted correspond with Luke Howard’s system of cloud categorization to some extent. Moreover, clouds painted by Constable are the easiest to classify (highest accuracy) with the classification accuracy of 0.8571. Additionally, in Fig. 11, we show the classification confusion matrices for each artist’s paintings. Constable’s clouds achieve the highest classification accuracy in the cumuliform and cumulonimbiform categories, which are most common in the collected dataset.

TABLE 3:  $\chi^2$ -statistic of z-test about the difference of classification accuracy.

Artist	$\chi^2$ -statistic	$p$ -value
Valenciennes	0.106	0.372
Watts	1.033	0.155
Lee	1.750	0.093
Lionel Constable	1.503	0.110
Boudin	3.456	0.032
Cox	3.290	0.035

To compare Constable with each of the other artists, we conducted hypothesis testing [58] with the alternative hypothesis: Constable’s paintings can be more accurately classified than the paintings of another artist. For clarity, we assign identification numbers 1 to Constable and 2, 3, ..., 7 to the other artists. We model the classification decision on a painting of the  $i$ th artist by a Bernoulli random variable with 1 indicating the correct classification and 0 otherwise. Let  $p_i$  be the probability of correct

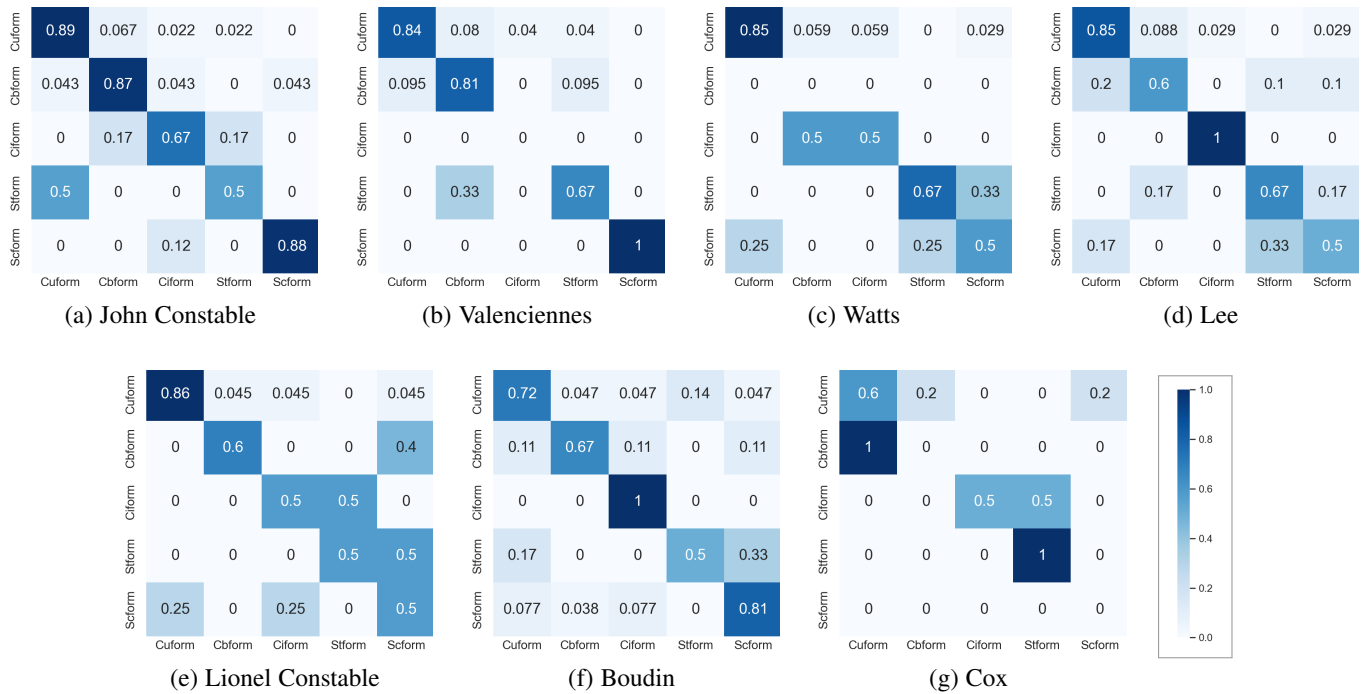


Fig. 11: The confusion matrices represent the classification results of all seven painters using the semi-supervised feature fusion model.

classification. Thus the distribution for the number of correctly classified paintings of artist  $i$  is a Binomial distribution. The null hypothesis is:  $p_1 \leq p_i, i \neq 1$ . We use the one-tail Z-test [59] with continuity correction. The  $p$ -values obtained are listed in Table 3. At the significance level 0.1, Constable’s paintings are more accurately classified than Lee, Boudin, and Cox, but not Valenciennes, Watts, or Lionel Constable.

We conducted the same hypothesis testing to examine whether adding edge features significantly improves the classification accuracy for any artist. The lowest  $p$ -value is obtained for Constable at 0.157, while the  $p$ -values for the other artists are all above 0.3. This result indicates that the edge features improved classification most significantly for Constable.

Based on the result, it is evident that Constable’s clouds correspond well with the system of cloud typology produced by Luke Howard. The 5% confidence interval for the classification accuracy of Constable’s paintings is  $[0.782, 0.932]$ , which is substantially above 50%. In addition, the average classification accuracy is highest for Constable’s paintings. Are Constable’s clouds more similar to photographs of real-world clouds compared to his contemporaries? The answer is mixed. At the significance level 0.1, a higher similarity is confirmed when compared to Lee, Boudin, and Cox, but not with Valenciennes, Watts, and Lionel Constable. One reason we are unable to confirm higher similarity in the case of the last three artists is that they each have a relatively small number of paintings available in the analysis.

We posit that Constable’s technique, which involves strong contour lines rendered with a relatively continuous brushstroke, contributes to the realism of his clouds. Some painters, such as Boudin, tended to use dots and dashes to replace the clear-edged and smooth contours that define cloud shapes. Boudin’s technique, which was influential for the Impressionists, mutes the features that differentiate cloud types. Yet Boudin’s contemporaries were just as wowed by the apparent truth of his painted clouds as Constable’s first French admirers had been by his back in 1824,

nearly 40 years earlier. In fact, Boudin was known in his lifetime as the “king of skies” [43]. Nevertheless, the computer—trained using photographs—finds Constable’s clouds easier to classify and, hence, to recognize. Constable was painting in the decades leading up to the invention of photography in 1839, when there was strong interest in empirically-based verisimilitude. Attention to precisely the morphological differences that Luke Howard used to create his typology of clouds in 1803 endowed Constable’s clouds with a sufficiently striking degree of realism to set him apart from other landscape painters, at least in the eyes of his contemporaries—and in the eyes of our CNN. Our findings cannot confirm definitively that Constable was familiar with Howard’s cloud classification, but they do confirm that systematic categorization is key for the visual impact of his realism.

## 5.4 Style Similarity Analysis

To train the style encoder for each artist, we used the MUNIT model [52] as the network backbone. We excluded Learning Regression loss during training as suggested by [42] for better disentanglement of content and style features. All the paintings of an artist form group  $\mathcal{A}$ , and a subset of real photos form group  $\mathcal{P}$  (See Fig. 8). We selected 300 real photos and ensured that the number of images in each cloud category is the same. For the paintings, instead of the original image, we used their sky-selected versions. After obtaining the style encoders, we can compute  $D_{\text{style}}$  and  $R_{\text{style}}$ .

### 5.4.1 Style Distance Between an Artist and Real Clouds

We computed  $R_{\text{style}}$  for each of the seven painters in our collection using Eq. (6). To assess variation in  $R_{\text{style}}$  caused by randomness in the input images, for each painter, we randomly sampled 5 paintings to form a group and computed  $R_{\text{style}}$  for this group. The calculation was repeated for multiple random samples of 5 paintings. As our collection only contains 9 paintings of Cox,

there are a maximum of 126 different combinations of 5 paintings from Cox. We thus randomly sampled subsets of 5 paintings 126 times for every artist. Table 4 shows the average values of  $R_{\text{style}}$  for each artist as well as the standard deviation.

To test whether these distances are significantly different for the artists, we conducted hypothesis testing [58] with the alternative hypothesis: these distances are significantly different between the artists. Denote the group of paintings for each of the seven artists by  $C_i$ ,  $i = 1, 2, \dots, 7$ , and the sampled subgroups by  $C_i^n$ ,  $n = 1, \dots, 126$ . Let the set  $\mathcal{R}_{\text{style}}(C_i) = \{R_{\text{style}}(C_i^n), n = 1, 2, \dots, 126\}$ . Assume that the distribution of  $R_{\text{style}}(C_i^n)$  for each group  $C_i$  is a Gaussian distribution  $N(\mu_i, \sigma_i^2)$ , where  $\mu_i$  and  $\sigma_i^2$  are the mean and variance. The null hypothesis is:  $\mu_1 = \mu_2, \dots, = \mu_7$ . We use the  $F$ -test for a one-way analysis of variance. The  $F$ -statistic is 21.15 with  $p$ -value below  $2e - 16$ . Thus the null hypothesis (the groups have the same mean value) is rejected at significance level 0.05. Then, we conducted another hypothesis test using  $T$ -test to test if paintings of Constable are more photo-like compared with other artists. If we use  $\mu_1$  to denote the mean value of Constable’s painting group. We conducted six hypothesis tests with the null hypothesis:  $\mu_1 \geq \mu_i$ ,  $i = 2, 3, \dots, 7$ . Table 5 shows the  $T$ -statistics and the corresponding  $p$ -values in each test. At significance level 0.1, the painting style of John Constable is more similar to photograph than Boudin’s, Lee’s, and Cox’s, while we cannot reject the null hypothesis that his painting style is less photo-like than Valenciennes’, Lionel Constable’s, and Watt’s. In addition, we conducted the same  $T$ -test to test whether on average  $R_{\text{style}}$  of Valenciennes is greater or equal to  $R_{\text{style}}$  of any other artist. All the  $p$ -values are below 0.1. This result suggests that Valenciennes’s painting style is most similar to real photos compared with the other six painters at the significance level 0.1. Furthermore, the Pearson correlation coefficient between the classification accuracy and style similarity is -0.782 ( $p$ -value is 0.039). This strong negative correlation between the measure of style difference (paintings versus photos) and the accuracy of cloud classification aligns well with our heuristics—paintings similar to photos being easier to classify into cloud types.

TABLE 4:  $R_{\text{style}}$  of the painting collection of each painter.

Artist	$R_{\text{style}}$ (mean $\pm$ std)
Valenciennes	1.163 $\pm$ 0.132
Lionel Constable	1.188 $\pm$ 0.141
John Constable	1.191 $\pm$ 0.147
Watts	1.210 $\pm$ 0.146
Boudin	1.254 $\pm$ 0.143
Lee	1.298 $\pm$ 0.151
Cox	1.319 $\pm$ 0.156

TABLE 5:  $T$  statistics of  $T$ -test about the difference of  $R_{\text{style}}$  between John Constable and other artists

Artist	$T$ -statistic	$p$ -value
Valenciennes	1.590	0.944
Lionel Constable	0.165	0.566
Watts	-1.029	0.152
Boudin	-3.448	3.310e-04
Lee	-5.699	1.689e-08
Cox	-6.703	6.775e-11

TABLE 6: Style distance among different painting collections.

Pair of Painting Collections in Comparison	$D_{\text{style}}$ (mean $\pm$ std)
(John Constable, John Constable)	0.351 $\pm$ 0.092
(John Constable, Lionel Constable)	0.359 $\pm$ 0.095
(John Constable, Valenciennes)	0.373 $\pm$ 0.109
(John Constable, Boudin)	0.405 $\pm$ 0.108
(John Constable, Cox)	0.408 $\pm$ 0.110
(John Constable, Watts)	0.421 $\pm$ 0.113
(John Constable, Lee)	0.439 $\pm$ 0.102
(John Constable:oil, John Constable:watercolor)	0.606 $\pm$ 0.143
(John Constable, Benton)	0.835 $\pm$ 0.149
(John Constable, Titian)	0.843 $\pm$ 0.138
(John Constable, Kinkade)	0.881 $\pm$ 0.156
(John Constable, O’Keeffe)	0.926 $\pm$ 0.153

TABLE 7:  $T$  statistics of  $T$ -test about the difference of  $D_{\text{style}}$

Artist	$T$ -statistic	$p$ -value
Lionel Constable	-0.679	0.249
Valenciennes	-1.730	0.042
Boudin	-4.270	1.387e-05
Cox	-4.462	6.225e-06
Watts	-5.390	8.312e-08
Lee	-7.190	3.797e-12
John Constable-watercolors	-16.834	<2.2e-16
Benton	-31.025	<2.2e-16
Titian	-33.298	<2.2e-16
Kinkade	-32.849	<2.2e-16
O’Keeffe	-36.153	<2.2e-16

#### 5.4.2 Style Similarity Between Painting Collections of Constable and His Contemporaries

Next, we use Eq. (3) to compute the style similarity between the painting collections of pairs of painters. The results are shown in Table 6. Again, we conducted hypothesis testing to verify whether these style distances are significantly different. We use  $C_1$  to denote the set of paintings by John Constable, and  $C_i$  to denote those of any other artist  $i$ . Similarly as in the previous subsection, we computed  $D_{\text{style}}$  between randomly sampled subsets of paintings by two artists. The same subsets used to generate  $R_{\text{style}}$  are used here. For the pair of groups  $C_1$  and  $C_i$ , we obtain 126 values of  $D_{\text{style}}$ :  $\mathcal{D}_{\text{style}}(C_1, C_i) = \{D_{\text{style}}(C_1^n, C_i^n), n = 1, 2, \dots, 126\}$ . To create a yardstick for comparison, we also computed  $D_{\text{style}}$  for subsets of paintings within Constable’s collection. Specifically, in addition to the 126 subsets  $C_1^n$  already created, another 126 random subsets were sampled from  $C_1$ , each containing 5 paintings. Denote these new subsets by  $C_{1,2nd}^n$ ,  $n = 1, \dots, 126$ . Then  $\mathcal{D}_{\text{style}}(C_1, C_1) = \{D_{\text{style}}(C_1^n, C_{1,2nd}^n), n = 1, 2, \dots, 126\}$ . If Constable is significantly different from the other artists in the sense of  $D_{\text{style}}$ , we expect the values in  $\mathcal{D}_{\text{style}}(C_1, C_i)$ ,  $i \neq 1$ , to be greater, at least on average, than those in  $\mathcal{D}_{\text{style}}(C_1, C_1)$ .

Denote the mean of  $\mathcal{D}_{\text{style}}(C_1, C_i)$  by  $\mu'_i$ . In the first test, the null hypothesis is:  $\mu'_1 = \mu'_2, \dots, = \mu'_7$ . Similarly, we use the  $F$ -test for one-way analysis of variance. The  $F$ -statistic obtained is 12.69 with a  $p$ -value of  $9.21e - 14$ , suggesting that there are significant differences between the style features of these paired artists.

Besides the seven painters discussed so far, we expanded



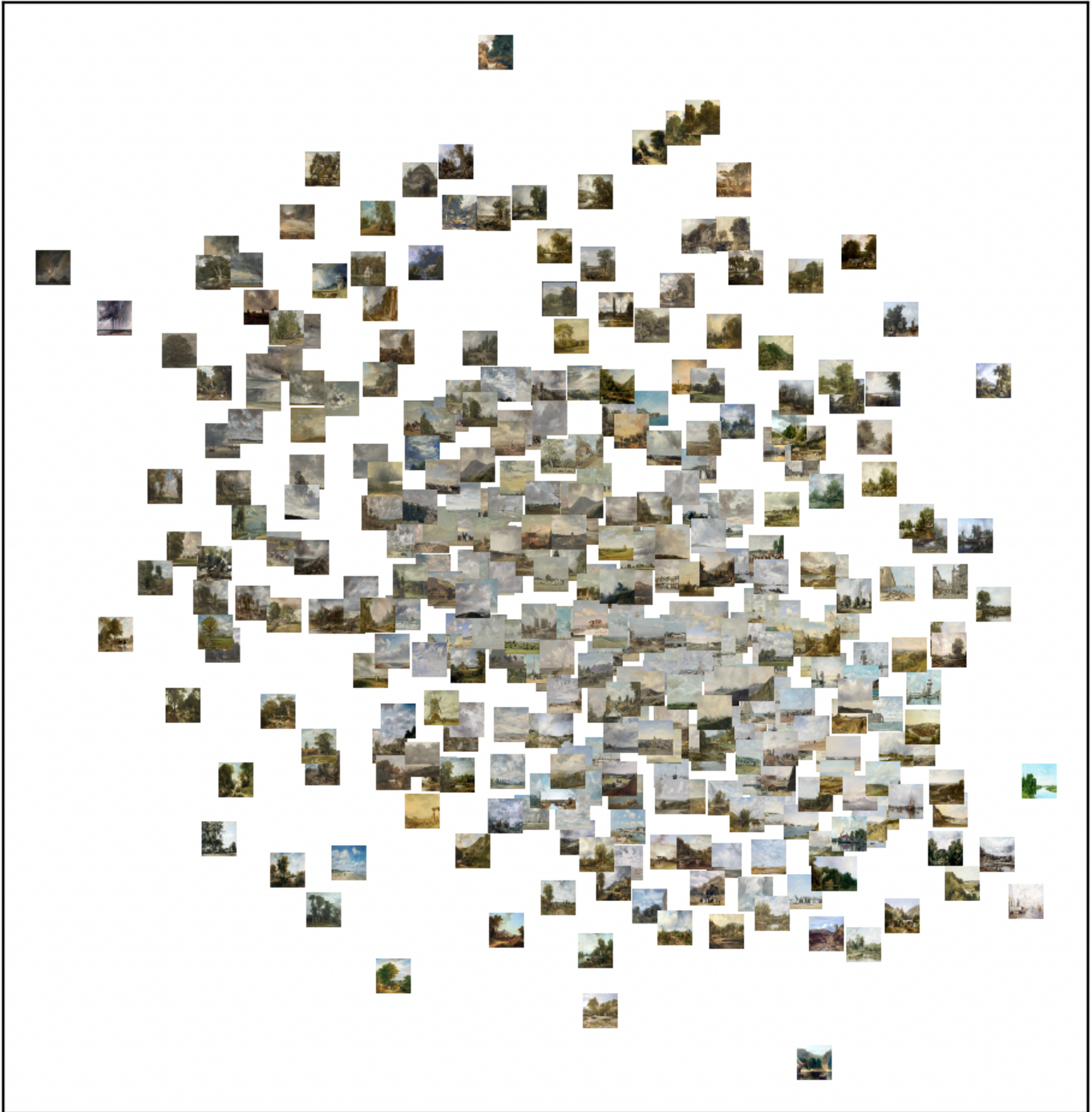


Fig. 12: Multidimensional scaling (MDS) results of paired paintings. MDS result showing all 363 painting. Only the sky regions are used in the analysis.

our dataset to include landscape paintings by artists working in diverse styles from the Renaissance painter Titian (c. 1490-1576), to the 20th-century modernists Georgia O’Keeffe (1887-1986) and Thomas Hart Benton (1889-1975), and the popular contemporary landscapist Thomas Kinkade (1958-2012) as well as watercolors by John Constable to show that the proposed style distance can be applied to more artists and media. The style distances between these artists and John Constable are provided in Table 6. We also conducted T-test between two data sets  $\mathcal{D}_{\text{style}}(C_1, C_1)$  and  $\mathcal{D}_{\text{style}}(C_1, C_i)$ , where  $i \in (2, \dots, 11)$  to test if artist  $i$ ’s painting style

is similar to John Constable’s. The null hypothesis is:  $\mu_1 \geq \mu_i$ ,  $i \neq 1$ . We test at the confidence level of 0.95. The  $T$ -statistic and the corresponding  $p$ -value for the 11 tests are listed in Table 7, and we can observe  $p$ -values are all below 0.05 except Lionel Constable. These statistics mean that, with the exception of Lionel Constable, John Constable’s paintings are different from other painters in terms of painting style at the significance level of 0.05. We can claim that Lionel Constable’s paintings have a more similar style to John Constable’s. In addition, to better understand the style distances between individual paintings in the entire

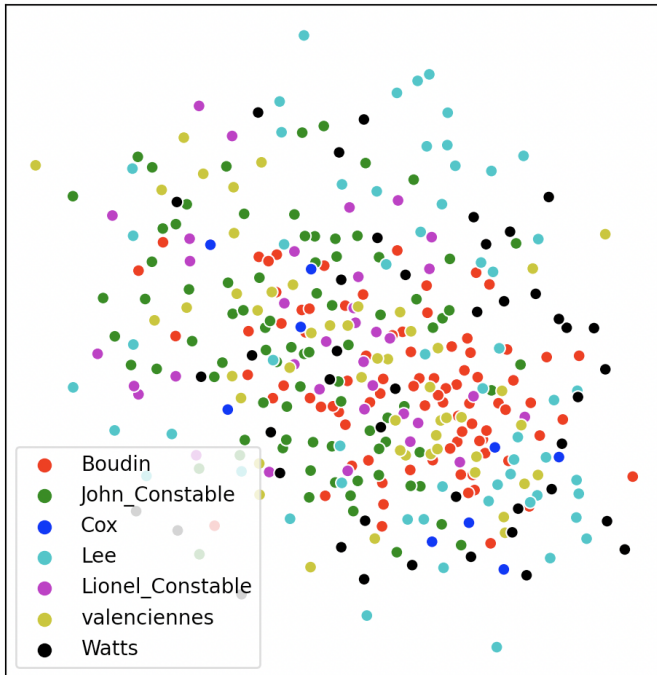


Fig. 13: Multidimensional scaling results of paired paintings, in the same way as in Fig. 12. Colors of the scattered points indicate different painters.

collection, we generate two figures to show the multidimensional scaling (MDS) results of these paintings using the style distances between any pair of paintings (Eq. (3) applied to groups each containing a single painting). Fig. 12 and 13 show the MDS result in two dimensions.

## 5.5 Art Historical Findings Based on Experimental Results

Based on the experimental results of cloud classification and style similarity measurement, we can summarize the key findings as follows:

- 1) John Constable’s clouds can be more accurately classified than his contemporaries, which sustains the possibility that Constable possessed some knowledge of Luke Howard’s classification of clouds but does not confirm it.
- 2) Fusing edge features boost the classification performance of Constable’s cloud more than others. This suggests that the well-defined structure of Constable’s clouds is an important factor for their realism.
- 3) John Constable’s paintings are not the most realistic of those tested if realism is defined by relative approximation of the appearance of a photograph. Valenciennes, according to our experiments, produced the most photo-like skies.
- 4) Lionel Constable is closest in painting style to John Constable, which is consistent with his known practice of emulating his father.

## 6 CONCLUSION

Moving beyond investigating this artistic movement solely through traditional methods of art history or via computer-aided stylistic analysis, we engage with meteorology both as a means of

gaining ground truth and as a historical discipline that may have influenced visual arts. Following the assumption that the more naturalistic the cloud painting is, the easier it is for the AI to determine its cloud type, we developed a new, specialized computer-based cloud type classification method to determine if Constable’s clouds or those of his contemporaries can be correctly categorized into different cloud types with a CNN model trained with real cloud photos from an explainable and interdisciplinary perspective by exploring the relationship between photos and paintings with expert annotations. The proposed feature fusion model is adopted for cloud type classification on a carefully-curated dataset containing oil paintings collected from seven renowned painters who were all adept at cloud studies. The classification results show that Constable’s clouds achieve the highest classification accuracy and are more likely to follow the accurate cloud structure. The improvement of the classification performance by fusing the edge features to the model reflects that Constable’s ability to depict the flat cloud base and curved cloud turrets is a key factor for his achievement of realistic cloud paintings. Additionally, we utilize two matrices to evaluate the style distance between paintings and photos and style similarity among these painters. The experimental statistics show that Constable’s paintings do not have the most similar style with real photos, although the classification accuracy is highest in Constable’s collection. The distance of style also demonstrates that Lionel Constable’s painting style is more similar to John Constable’s.

Further avenues for art historical inquiry are indicated by our research. For one thing, the stylistic similarity between Valenciennes and Constable invites a reconsideration of their relationship. There is no record of their meeting, and the younger Constable’s direct encounter with Valenciennes’ cloud studies is unattested. The two artists did have mutual friends and acquaintances, though, and Constable may have learned of the older artist’s plein air technique for depicting clouds through this network. Also possible is that the two artists are registering with equal force a growing predilection around 1800 in Europe and Britain for a mode of naturalism that was ultimately satisfied by the invention of photography in 1839. Our experiments, in fact, suggest that even artists closely associated with naturalism like Boudin were working in a less photographic mode than like-minded predecessors who died just before photography was invented. This raises the interesting possibility that a kind of photographic realism was highly prized around 1800, but soon seen as less realistic when applied to painting once photographs were more or less ubiquitous after the 1850s. These possibilities can be investigated further using the style similarity analysis here presented.

## ACKNOWLEDGMENTS

This material is based upon work supported by the National Endowment for the Humanities (NEH) under Grant No. HAA-271801-20. Any views, findings, conclusions, or recommendations expressed in this article do not necessarily represent those of the NEH. This work used the Extreme Science and Engineering Discovery Environment (XSEDE), which is supported by the National Science Foundation Grant No. ACI-1548562. J. Z. Wang’s research was supported by generous gifts from the Amazon Research Awards program. Xinye Zheng and Kevin R. Victor contributed in the early stage of the project. The authors would like to thank the Yale Center for British Art for hosting a visit of the team and for valuable discussions.

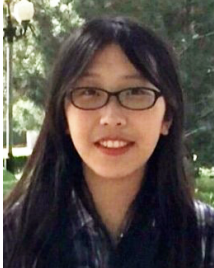
## REFERENCES

- [1] E. A. Payne, *Composition of Outdoor Painting*. EP Payne, 1957.
- [2] D. G. Stork, "Optics and realism in Renaissance art," *Scientific American*, vol. 291, no. 6, pp. 76–83, 2004.
- [3] S. Lyu, D. Rockmore, and H. Farid, "A digital technique for art authentication," *Proceedings of the National Academy of Sciences*, vol. 101, no. 49, pp. 17 006–17 010, 2004.
- [4] J. Li, L. Yao, E. Hendriks, and J. Z. Wang, "Rhythmic brushstrokes distinguish Van Gogh from his contemporaries: Findings via automated brushstroke extraction," *IEEE Transactions on Pattern Analysis and Machine Intelligence*, vol. 34, no. 6, pp. 1159–1176, 2012.
- [5] J. Z. Wang, B. Kandemir, and J. Li, "Computerized analysis of paintings," in *The Routledge Companion to Digital Humanities and Art History*. Routledge, 2020, pp. 299–312.
- [6] L. Howard, *Essay on the Modifications of Clouds*. John Churchill & Sons, 1803.
- [7] K. Badt, *John Constable's Clouds*. Taylor & Francis, 1950.
- [8] A. Chamberlain, *John Constable*. George Bell & Sons, 1903.
- [9] L. Hawes, "Constable's sky sketches," *Journal of the Warburg and Courtauld Institutes*, pp. 344–365, 1969.
- [10] J. E. Thorne and J. Constable, *John Constable's Skies: A fusion of art and science*. A&C Black, 1999.
- [11] G. Reynolds, "Constable's skies," in *Constable's Skies*, F. Bancroft, Ed. New York: Salander-O'Reilly Galleries, 2004, pp. 19–27.
- [12] K. Fukushima and S. Miyake, "Neocognitron: A self-organizing neural network model for a mechanism of visual pattern recognition," in *Competition and Cooperation in Neural Nets*. Springer, 1982, pp. 267–285.
- [13] Y. LeCun, P. Haffner, L. Bottou, and Y. Bengio, "Object recognition with gradient-based learning," in *Shape, Contour and Grouping in Computer Vision*. Springer, 1999, pp. 319–345.
- [14] Y. Bar, N. Levy, and L. Wolf, "Classification of artistic styles using binarized features derived from a deep neural network," in *Proceedings of the European Conference on Computer Vision (ECCV)*. Springer, 2014, pp. 71–84.
- [15] W.-T. Chu and Y.-L. Wu, "Image style classification based on learnt deep correlation features," *IEEE Transactions on Multimedia*, vol. 20, no. 9, pp. 2491–2502, 2018.
- [16] N. Westlake, H. Cai, and P. Hall, "Detecting people in artwork with cnns," in *Proceedings of the European Conference on Computer Vision (ECCV)*. Springer, 2016, pp. 825–841.
- [17] H. Lin, M. V. Zuijlen, M. W. Wijntjes, S. C. Pont, and K. Bala, "Insights from a large-scale database of material depictions in paintings," in *Proceedings of the International Conference on Pattern Recognition*. Springer, 2021, pp. 531–545.
- [18] H. Mao, M. Cheung, and J. She, "Deepart: Learning joint representations of visual arts," in *Proceedings of the 25th ACM International Conference on Multimedia*, 2017, pp. 1183–1191.
- [19] S. Shaik, B. Bucher, N. Agrafiotis, S. Phillips, K. Daniilidis, and W. Schmenner, "Learning portrait style representations," *arXiv preprint arXiv:2012.04153*, 2020.
- [20] I. Goodfellow, J. Pouget-Abadie, M. Mirza, B. Xu, D. Warde-Farley, S. Ozair, A. Courville, and Y. Bengio, "Generative adversarial nets," *Advances in Neural Information Processing Systems*, vol. 27, p. 2672–2680, 2014.
- [21] D. Kotovenko, A. Sanakoyeu, S. Lang, and B. Ommer, "Content and style disentanglement for artistic style transfer," in *Proceedings of the IEEE/CVF International Conference on Computer Vision*, 2019, pp. 4422–4431.
- [22] Z. Huang, W. Heng, and S. Zhou, "Learning to paint with model-based deep reinforcement learning," in *Proceedings of the IEEE/CVF International Conference on Computer Vision*, 2019, pp. 8709–8718.
- [23] J. Lawson-Tancred, "Enigma machines," *Apollo*, pp. 34–36, December 2021.
- [24] A. C. Esmeijer, "Cloudscapes in theory and practice," *Simiolus: Netherlands Quarterly for the History of Art*, vol. 9, no. 3, pp. 123–148, 1977.
- [25] A. Lyles, "This glorious pageantry of heaven," in *Constable's Skies*, F. Bancroft, Ed. New York: Salander-O'Reilly Galleries, 2004, pp. 29–54.
- [26] M. Šinko, P. Kamencay, P. Šỳkora, M. Benčo, and R. Hudec, "Cloud-type classification of ground-based images using deep learning," in *Proceedings of the 17th International Conference on Emerging eLearning Technologies and Applications (ICETA)*. IEEE, 2019, pp. 715–720.
- [27] T. Ojala, M. Pietikainen, and T. Maenpää, "Multiresolution gray-scale and rotation invariant texture classification with local binary patterns," *IEEE Transactions on Pattern Analysis and Machine Intelligence*, vol. 24, no. 7, pp. 971–987, 2002.
- [28] A. Heinle, A. Macke, and A. Srivastav, "Automatic cloud classification of whole sky images," *Atmospheric Measurement Techniques*, vol. 3, no. 3, pp. 557–567, 2010.
- [29] W. Zhuo, Z. Cao, and Y. Xiao, "Cloud classification of ground-based images using texture–structure features," *Journal of Atmospheric and Oceanic Technology*, vol. 31, no. 1, pp. 79–92, 2014.
- [30] S. Dev, Y. H. Lee, and S. Winkler, "Categorization of cloud image patches using an improved texton-based approach," in *Proceedings of the IEEE International Conference on Image Processing (ICIP)*. IEEE, 2015, pp. 422–426.
- [31] J. Zhang, P. Liu, F. Zhang, and Q. Song, "CloudNet: Ground-based cloud classification with deep convolutional neural network," *Geophysical Research Letters*, vol. 45, no. 16, pp. 8665–8672, 2018.
- [32] J. Huertas-Tato, A. Martín, and D. Camacho, "Cloud type identification using data fusion and ensemble learning," in *Proceedings of the International Conference on Intelligent Data Engineering and Automated Learning*. Springer, 2020, pp. 137–147.
- [33] D.-H. Lee, "Pseudo-Label: The simple and efficient semi-supervised learning method for deep neural networks," in *Proceedings of the Workshop on Challenges in Representation Learning, in conjunction with the International Conference on Machine Learning*, vol. 3, no. 2, 2013, p. 896.
- [34] X. Ning, X. Wang, S. Xu, W. Cai, L. Zhang, L. Yu, and W. Li, "A review of research on co-training," *Concurrency and Computation: Practice and Experience*, p. e6276, 2021.
- [35] S. S. Sawant and M. Prabukumar, "A review on graph-based semi-supervised learning methods for hyperspectral image classification," *The Egyptian Journal of Remote Sensing and Space Science*, vol. 23, no. 2, pp. 243–248, 2020.
- [36] H. Dong, L. Yang, and X. Wang, "Robust semi-supervised support vector machines with laplace kernel-induced coreentropy loss functions," *Applied Intelligence*, vol. 51, no. 2, pp. 819–833, 2021.
- [37] A. Chartsias, T. Joyce, G. Papanastasiou, S. Semple, M. Williams, D. E. Newby, R. Dharmakumar, and S. A. Tsafaris, "Disentangled representation learning in cardiac image analysis," *Medical Image Analysis*, vol. 58, p. 101535, 2019.
- [38] J. Charles, T. Pfister, D. Magee, D. Hogg, and A. Zisserman, "Domain adaptation for upper body pose tracking in signed TV broadcasts," in *Proceedings British Machine Vision Conference*. British Machine Vision Association, 2013.
- [39] G. Kwon and J. C. Ye, "Diagonal attention and style-based gan for content-style disentanglement in image generation and translation," *arXiv preprint arXiv:2103.16146*, 2021.
- [40] H.-Y. Lee, H.-Y. Tseng, J.-B. Huang, M. Singh, and M.-H. Yang, "Diverse image-to-image translation via disentangled representations," in *Proceedings of the European Conference on Computer Vision (ECCV)*, 2018, pp. 35–51.
- [41] M.-Y. Liu, T. Breuel, and J. Kautz, "Unsupervised image-to-image translation networks," in *Advances in Neural Information Processing Systems*, 2017, pp. 700–708.
- [42] X. Liu, S. Theros, G. Valvano, A. Chartsias, A. O'Neil, and S. A. Tsafaris, "Metrics for exposing the biases of content-style disentanglement," *arXiv preprint arXiv:2008.12378*, vol. 7, 2020.
- [43] C. Sterling, *French Paintings: A Catalogue of the Collection of The Metropolitan Museum of Art. Vol. 3, Nineteenth and Twentieth Centuries*. Metropolitan Museum of Art, 1967.
- [44] J. Li, "Agglomerative connectivity constrained clustering for image segmentation," *Statistical Analysis and Data Mining: The ASA Data Science Journal*, vol. 4, no. 1, pp. 84–99, 2011.
- [45] K. He, X. Zhang, S. Ren, and J. Sun, "Deep residual learning for image recognition," in *Proceedings of the IEEE Conference on Computer Vision and Pattern Recognition*, 2016, pp. 770–778.
- [46] K. P. Murphy, *Machine Learning: A Probabilistic Perspective*. MIT press, 2012.
- [47] R. R. Selvaraju, M. Cogswell, A. Das, R. Vedantam, D. Parikh, and D. Batra, "Grad-cam: Visual explanations from deep networks via gradient-based localization," in *Proceedings of the IEEE International Conference on Computer Vision*, 2017, pp. 618–626.
- [48] S. Xie and Z. Tu, "Holistically-nested edge detection," in *Proceedings of the IEEE International Conference on Computer Vision*, 2015, pp. 1395–1403.
- [49] R. P. Mihail, S. Workman, Z. Bessinger, and N. Jacobs, "Sky segmentation in the wild: An empirical study," in *2016 IEEE Winter Conference on Applications of Computer Vision (WACV)*. IEEE, 2016, pp. 1–6.
- [50] S. Rawat, S. Gairola, R. Shah, and P. Narayanan, "Find me a sky: A data-driven method for color-consistent sky search and replacement," in



*Proceedings of the International Conference on Multimedia Modeling*. Springer, 2018, pp. 216–228.

- [51] K. Sohn, D. Berthelot, C.-L. Li, Z. Zhang, N. Carlini, E. D. Cubuk, A. Kurakin, H. Zhang, and C. Raffel, “Fixmatch: Simplifying semi-supervised learning with consistency and confidence,” *arXiv preprint arXiv:2001.07685*, 2020.
- [52] X. Huang, M.-Y. Liu, S. Belongie, and J. Kautz, “Multimodal unsupervised image-to-image translation,” in *Proceedings of the European Conference on Computer Vision (ECCV)*, 2018, pp. 172–189.
- [53] B. Zhou, H. Zhao, X. Puig, S. Fidler, A. Barriuso, and A. Torralba, “Scene parsing through ade20k dataset,” in *Proceedings of the IEEE Conference on Computer Vision and Pattern Recognition*, 2017, pp. 633–641.
- [54] Z. Wang, E. Wang, and Y. Zhu, “Image segmentation evaluation: A survey of methods,” *Artificial Intelligence Review*, vol. 53, no. 8, pp. 5637–5674, 2020.
- [55] L. Perez and J. Wang, “The effectiveness of data augmentation in image classification using deep learning,” *arXiv preprint arXiv:1712.04621*, 2017.
- [56] M. Hossin and M. Sulaiman, “A review on evaluation metrics for data classification evaluations,” *International Journal of Data Mining & Knowledge Management Process*, vol. 5, no. 2, p. 1, 2015.
- [57] E. Barrett and C. Grant, “The identification of cloud types in LANDSAT MSS images,” *ERTS Follow-on Programme Study Report, U.K. Department of Industry*, 1976. [Online]. Available: <https://ntrs.nasa.gov/citations/19760014556>
- [58] C. Pernet, “Null hypothesis significance testing: a short tutorial,” *F1000Research*, vol. 4, 2015.
- [59] S. Suissa and J. J. Shuster, “Are uniformly most powerful unbiased tests really best?” *The American Statistician*, vol. 38, no. 3, pp. 204–206, 1984.

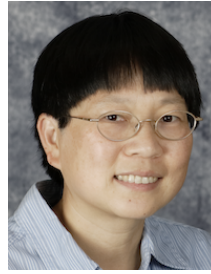


**Zhuomin Zhang** is a Ph.D. candidate in the College of Information Sciences and Technology at The Pennsylvania State University, where she closely works with her advisors Drs. James Z. Wang and Jia Li. Her research interests mostly lie in computer vision, machine learning, and multimedia. She received her bachelor’s degree in Computer Science from Nanjing University in 2016.



**Elizabeth Mansfield** is Professor of Art History and Head of the Department of Art History at Penn State. A specialist in 18th- and 19th-century European art and art historiography, her publications include the books *The Perfect Foil: François-André Vincent and the Revolution in French Painting* and *Too Beautiful to Picture: Zeuxis, Myth, and Mimesis*. The latter was awarded the Charles Rufus Morey book prize by the College Art Association in 2008.

Past positions include academic appointments at New York University and at Sewanee: The University of the South. Prior to joining the faculty at Penn State in 2018, she served as Senior Program Officer at the Getty Foundation and Vice President for Scholarly Programs at the National Humanities Center. Her current book project is a study of Realism.



**Jia Li** is a Professor of Statistics and (by courtesy) Computer Science at The Pennsylvania State University. Her research interests include machine learning, artificial intelligence, probabilistic graph models, and image analysis. She worked as a Program Director at the National Science Foundation from 2011 to 2013, a Visiting Scientist at Google Labs in Pittsburgh from 2007 to 2008, a researcher at the Xerox Palo Alto Research Center from 1999 to 2000, and a Research Associate in the Computer Science Department at Stanford University in 1999. She received the M.Sc. degree in Electrical Engineering (1995), the M.Sc. degree in Statistics (1998), and the Ph.D. degree in Electrical Engineering (1999), from Stanford University. She was Editor-in-Chief for *Statistical Analysis and Data Mining: The ASA Data Science Journal* from 2018 to 2020. She is a Fellow of the Institute of Electrical and Electronics Engineers and a Fellow of the American Statistical Association.



**John Russell** is Assistant Professor and Digital Humanities Librarian at The Pennsylvania State University Libraries and Associate Director of the Center for Virtual/Material Studies. He holds a B.A. from the University of Vermont and an MLS from Indiana University.



**George Young** is a Professor of Meteorology at The Pennsylvania State University. His research interests are observational and statistical meteorology on scales ranging from individual clouds to large-scale weather systems. His contributions include participation in the planning, execution, and data analysis of numerous observational programs. His computational research involves the application of statistics, optimization, and machine learning to weather forecasting, satellite cloud image typing, and a range of interdisciplinary problems. He has been a member of the Penn State faculty since 1986. He received an MS degree in Meteorology (1982) from Florida State University and a PhD degree in Atmospheric Science (1986) from Colorado State University. He is a Fellow of the American Meteorological Society.



**Catherine Adams** worked as the assistant curator of the Visual Resources Centre in the Department of Art History at The Pennsylvania State University from 2007 until 2021, when she became Digital Support Specialist in the new Center for Virtual/Material Studies. She has experience in metadata and digital image creation and curation. She has managed the Art History Department Visual Resource Collection and the Palmer Museum of Art’s online collections in CONTENTdm. She aided in the creation of Arts

and Architecture Resource Collaborative (AARC) and in several Omeka and Omeka S sites. She holds a B.A. from The Pennsylvania State University and an MLIS from the University of Pittsburgh.





**James Z. Wang** is a Distinguished Professor of the Data Sciences and Artificial Intelligence section of the College of Information Sciences and Technology at The Pennsylvania State University. He received the bachelor's degree in mathematics *summa cum laude* from the University of Minnesota, and the MS degree in mathematics, the MS degree in computer science, and the PhD degree in medical information sciences, all from Stanford University. His research interests include image analysis, image modeling, image

retrieval, and their applications. He was a visiting professor at the Robotics Institute at Carnegie Mellon University (2007-2008), a lead special section guest editor of the IEEE Transactions on Pattern Analysis and Machine Intelligence (2008), and a program manager at the Office of the Director of the National Science Foundation (2011-2012). He is on the editorial board of the IEEE BITS – The Information Theory Magazine's special issue on Information Processing in Arts and Humanities (2022). He was a recipient of a National Science Foundation Career award (2004) and Amazon Research Awards (2018, 2019, 2020).